

Effect of High Strength Steel Microstructure on Crack Tip Opening Displacement

Enefola S. Ameh¹, Basil O. Onyekpe²

¹(Department Of Mechanical Engineering, University Of Benin, Nigeria)

²(Department Of Mechanical Engineering, University Of Benin, Nigeria)

ABSTRACT: This study investigates the influence of high strength steel microstructure morphology on crack tip opening displacement (CTOD). Three different heat treatment methods (normalizing, austempering, quenching and tempering) were performed on the as-received steel at 950°C austenization temperature for 90minutes; the resulting microstructures characterized and crack tip opening displacement tests were conducted with compact tension specimens at room temperature as prescribed by American standard testing method (ASTM) E1820. Normalized microstructure resulted in the highest critical fracture toughness value of 0.2263mm, followed by quenched and tempered (0.1265mm), as-received (0.0877mm) and austempered microstructure (0.0546mm). The results indicated very significant microstructure morphology sensitivity to crack tip opening displacement and therefore provides a valuable parameter for correlating fracture toughness to microstructure.

Keywords: CTOD, fracture toughness, high strength steel, microstructure

I. INTRODUCTION

The Micro-alloyed steel with yield strength between 350 to 700MPa is termed high strength steel [1]. High strength steels have found wide application in offshore structures, like mooring attachment for floating structures such as tension leg platform, pipelines, jacket structures and topsides [2]. The use of high strength steel offers a lot of advantages in terms of lower weight, lower manufacturing costs due to reduced amount of welding and ease of handling and transportation but it has been reported to be highly susceptible to crack formation during welding, fabrication and installation and sometimes in-service due to inherent high hardenability and influence of alloying elements despite its useful property [3]. The presence of crack can seriously reduce reliability of structures and components in-service [4]. Crack and fracture remain a problem the society would continue to face provided there are man-made- structures and components [5]. Several structural failures due to inherent low fracture toughness have been reported mainly in the oil and gas industry despite numerous literature reviews on microstructure of the high strength steel [6].

Material resistance to fracture is characterized by fracture toughness to define materials ability containing a crack to oppose fracture and crack tip opening displacement(CTOD) is one of the fracture mechanic parameters for predicting fracture toughness of a cracked structure [7, 8]. The CTOD can be calculated by summing up both the elastic and plastic components. The elastic component is calculated from the applied stress intensity factor, while the plastic component is calculated from CMOD [9]:

$$CTOD(\delta) = \frac{4}{\pi} \frac{k_I^2}{E\sigma_{ys}} = \frac{4G}{\pi\sigma_{ys}} \quad (1)$$

$$CTOD(\delta) = \frac{K_I^2}{E\sigma_{ys}} = \frac{G}{\sigma_{ys}} \quad (2)$$

The general experimental estimation for total CTOD is given by:

$$CTOD(\delta) = \delta_e + \delta_p = \frac{K^2(1-\nu^2)}{2E\sigma_{ys}} + \frac{r_p(w-a)v_p}{r_p(w-a)+a+z} \quad (3)$$

w =specimen width, a = crack length, ν = poisons ratio, ν_p = plastic component of CMOD that correspond to the critical load, z = knife edge distance and τ_p = plastic rotation that is usually approximated as 0.44 and 0.46 for SENB and CT specimen respectively.

The microstructure of high strength steel and its relationship to fracture toughness is very complex and are being influenced by composition and heat treatment methods [10]. The effect and importance of microstructure relation to fracture toughness of steel is widely acknowledged and still have contradictory literatures because of complexity with microstructural phases, constituents formation mechanism, and in addition to the fact that different microstructure offers different combination of strength and toughness for the same chemical composition [11]. In this study, effect of high strength steel microstructure morphology on crack tip opening displacement was investigated with a view to improving understanding of microstructural constituents influence on mechanical properties and developing high performance steel that will enhance steel design, lower weight and lower manufacturing cost in the oil and gas industry.

II. EXPERIMENTAL PROCEDURES

2.1 Material and Heat Treatments

Material used in the research work was 25mm thick plate of high strength steel and was procured from Masteel Company in UK. Optical emission spectroscopy analysis was conducted as prescribed by ASTM E415-14 to obtain the chemical composition of the as-received steel and the result revealed - 0.161% carbon, 0.296% silicon, 1.3% manganese, 0.011% phosphorus, 0.0006% sulphur, 0.0042% nitrogen, 0.03% copper, 0.11% molybdenum, 0.051% nickel, 0.062% chromium, 0.002% vanadium, 0.026% niobium, 0.004% titanium, 0.0017% boron, 0.076% aluminum and the remaining percentage for iron agreed with the chemical composition supplied by the Company. All specimens were cut from the high strength steel plate and machined to sizes slightly larger than the compact tension specimen's geometry prescribed by ASTM E1820 standard and then machined to final dimensions after heat treatments. Heat treatments such as normalizing, austempering and quenching and tempering were performed at 950°C austenization temperature and 90minutes isothermal holding time. The sample for quenching and tempering was tempered to 550°C in a furnace and held for 90minutes while the austempered sample was quenched in a salt bath electric resistance furnace of molten or fluidized potassium chloride (KCL) and Barium chloride (BaCl₂) at 2:1 mole ratio and maintained at 350°C for ninety minutes before being cooled in ambient temperature.

2.2 Crack Tip Opening Displacement Tests

CTOD test was performed as prescribed by ASTM E1820 "Standard Test Method for Measurement of Fracture Toughness." [12]. Specimens' preparation and the formulae used for the experimental analysis were taken from the standard. The compact tension geometry is indicated in Fig 1 while the dimensions are listed in Table 1. Four compact tension (CT) specimens were machined to normal width (W), followed by fatigue pre-cracking to a/W of approximately 0.5 to create the initial crack size and then side grooved both sides of the specimen to 10% on each side equaling total normal thickness reduction of 20% to ensure a straight crack front. Tests were performed on a servo hydraulic machine (Fig 2) equipped with a pair of clevises with pair of pins for loading specimen and displacement gage for measuring specimen's crack opening displacement. The tests were controlled through automated computer attached to the machine and the load and COD were continuously monitored and the crack lengths were measured through compliance relationship with the following mathematical relationships [12]:

$$\frac{a_i}{W} = 1.00196 - 4.06319U + 11.242U^2 - 106.043U^3 + 464.335U^4 - 650.677U^5 \quad (4)$$

where, $U = \frac{1}{(BEC_i)^{1/2} + 1}$, which is non-dimensional crack mouth opening displacement

B_e =effective thickness = $B - \left(\frac{B-BN}{B}\right)^2$, $C_i = \Delta V / \Delta P$ =Compliance.

The CTOD (δ) for each current crack length a_i was calculated as prescribed by ASTM E1820]:

$$\delta = \frac{J}{m\sigma_y} = \left[k_1^2 \frac{(1-\nu^2)}{E} + J_{pl} \right] = \frac{k_{(i)}^2 (1-\nu^2)/E}{m\sigma_y} + J_{pl(i)} \quad (5)$$

Where, m is a constant, σ_y is material yield, strength stress intensity factor, $k_i = \frac{P}{(BBNW)^{1/2}} f\left(\frac{a_i}{W}\right)$; plastic component of current crack length, $J_{pl(i)} = \left[J_{pl(i-1)} + \left(\frac{\eta_{pl}}{B^{(i-1)}}\right) (A_{pl(i)} - A_{pl(i-1)}) (1 - \gamma_{pl}) \left(\frac{a_i - a_{(i-1)}}{b^{(i-1)}}\right) \right]$
 $\eta_{pl} = 3.667 - 2.199(a_i/W) + 0.437(a_i/W)^2$, $\gamma_{pl} = 0.131 + 2.131(a_i/W) - 1.465(a_i/W)^2$, Area plastic component, $A_{pl(i)} = A_{pl(i-1)} + [P_{(i)} + P_{(i-1)}][V_{pl(i)} + V_{pl(i-1)}]/2$

Table 1: CT specimen dimension

| Quantity | Measured value (mm) |
|------------------------------------|----------------------------------|
| Specimen height (H) | 1.2*W = 30.50 |
| Specimen width (W) | 25.40 |
| Specimen thickness (B) | 0.5*W = 12.70 |
| Crack length (notch + pre-cracked) | 0.45 ≤ a _o /W ≤ 0.55. |
| Notch Length (n) | 0.25*W = 6.35 |
| Pre-cracking length (L) | 0.05B = 0.64 |
| Notch height (N) | 0.1*W = 2.54 |
| Span length (S) | 0.55*W = 13.97 |
| Pin hole diameter (d) | 0.25*W = 6.35 |
| Total specimen length (T) | 1.25*W = 31.75 |

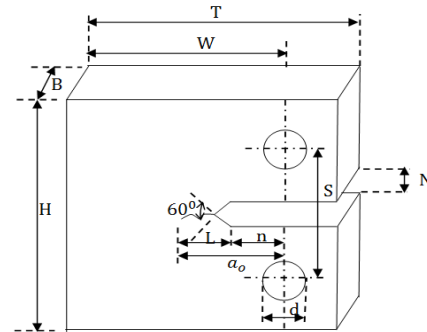


Figure 1: CT specimen geometry



Figure 2: Servohydraulic Machine for CTOD Test

2.3 Microstructure and Fracture Surface Characterization

Specimens were ground with emery (silicon carbide) papers in the order of decreasing coarseness of 120, 220, 600 and 1200 grit and then polished with 6 microns and 1 micron diamond paste respectively. Polished specimens were etched by dipping the surface into 2% nital (2% nitric acid and 95% ethanol) and then viewed under light optical fitted with digital camera and computer system. Fracture surfaces of the CTOD specimens were performed to characterize the failure mode and mechanism of the as-received and heat treated samples. Half of the broken fracture surfaces of specimens were examined using scanning electron microscope SEM at an accelerated voltage of 30KV.

III. RESULT AND DISCUSSIONS

3.1 Effect of Microstructure on CTOD

The resulting microstructure for the as-received steel and the different heat treated methods are shown in Fig 3. CTOD-Δa (Fig 4) resistance curves produced in accordance with ASTM E1820 indicated CTOD values increased linearly and then nonlinearly with crack extension and the critical fracture toughness values δ_{IC} calculated from the respective resistance curve. The CTOD values for the as received steel sample was 0.0877mm, 0.2263mm for normalized microstructure, 0.0546mm for austempered microstructure and 0.1265mm for

quenched and tempered microstructure. CTOD value of normalized microstructure indicated the highest fracture toughness. The increased in fracture toughness compared to the other steel samples was due to the microstructural constituents' makeup in the steel sample which revealed formation of soft ferrite matrix in the microstructure. The ferrite microstructural constituent improved toughness of steel by blunting the crack tips. The observation was in agreement with [13] finding that impact toughness of steel which had undergone normalization was made tougher than austempered, quenched and tempered steel.

The fracture toughness value of austempered microstructure was a little lower than the quenched and tempered microstructure. This finding was in contrast with [14] that toughness of alloying steel can be improved by replacing conventional quenching and tempering with austempering which has bainitic or mixed bainite-martensite microstructure instead of fully martensite structure. Large size of bainite sheaves observed in the austempered microstructure may have contributed to the low toughness by sharpening the tip of cracks. This implied bainite sheaves/plates are more sensitive to microcracking and could lead to brittle fracture due to their non-parallel sheaves formation depending on the grain sizes.

But the fracture toughness value of the quenched and tempered microstructure was a little less than normalized microstructure and higher than the as-received microstructure. Significant increase in fracture toughness witnessed in the quenched and tempered microstructure could be attributed to particle and dispersed cementite grains in ferritic matrix. Tempering steel containing alloy elements such as chromium, molybdenum, titanium, tungsten or vanadium had been reported to be strong carbide formers and precipitate as alloy carbide preferentially to cementite formation at temperature range of 550 to 600°C. The alloy element formed fine and dispersed carbide, and the dispersed alloy carbides will replace coarser cementite particles and remain small and dispersed even at elevated temperature because of their sluggish diffusion [15]. Deducing from the study, the precipitated carbides prevented grain growth by pinning down nucleation site during recovery of martensite laths and consequently leads to enhancement of fracture toughness. The study showed tempering temperature of 550°C at 90minutes holding time resulted in recrystallization and subsequent formation of ferrite, coarsening and partial spheroidization of cementite.

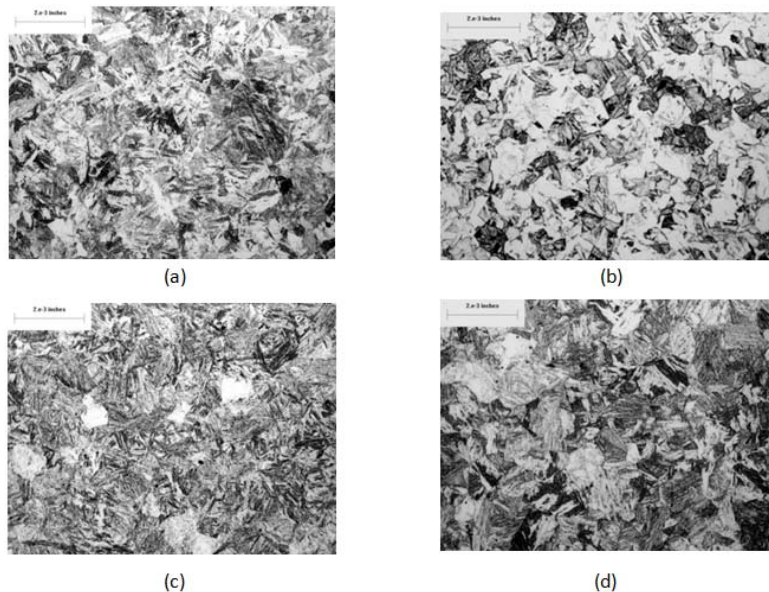


Figure 3: Microstructure (LOM X 1050)– **a)** As-received consist of martensite with traces of bainite, **b)** Normalized consist of ferrite/pearlite, **c)** Austempered consist of predominately lower bainite with traces of upper bainite sheaves, & **d)** Quenched and Tempered consist of blocks of martensite with traces of bainite.

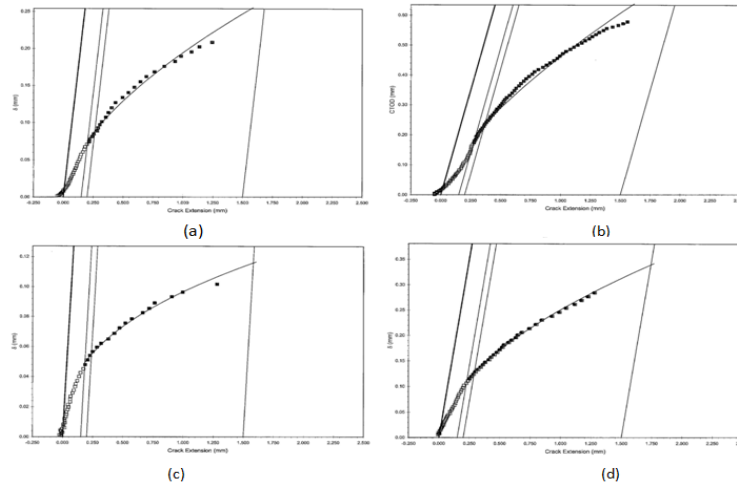


Figure 4: CTOD - Δa resistance curve- **a)** As-received, **b)** Normalized, **c)** Austempered & **d)** Quenched and Tempered steel

3.2 Fracture Surface Analysis

Fig 5(a) to 8(a) surfaces correspond to just ahead of fatigue precrack whereas Fig 5(b) through 8(b) zones correspond to middle of specimen fracture surface. Fig 5(a) to 8(a) showed small and shallow dimples fracture surface indicating low toughness even though the morphology appeared somehow ductile. The exhibited ductile morphology only proved the specimens showed small scale yielding at the crack tip. The results demonstrated the fracture surfaces just at the end of precrack exhibited ductile morphologies that was at variance with the remaining part of the fractures. Whereas the fracture surfaces (Fig 5b – 8b) contained tear ridges between cleavage facets which is associated with local ductile failure. The fracture surface morphologies were characterized with predominantly cleavage facets and showed very similar cleavage facets with little or no dimples which were indications the samples failed largely in cleavage mode and characteristic of profile of brittle fracture. However, normalized fracture surface indicated the finest cleavage facets size and this observation agreed with the CTOD test results that indicated normalized microstructure as the toughest of all the samples considered. The presence of unwanted inclusion observed in the micrographs (Fig 5b – 8b) could be explained with [6] the literature that small particle or non-metallic inclusions found in dimples may be attributed to either because they were separated from specimen during fracture or they were adhered to the dimples on the other half specimen. The observed inclusions could had played significant role in fracture toughness level of the samples investigated and its effect could even be more pronounced if the inclusions are connected to each other.

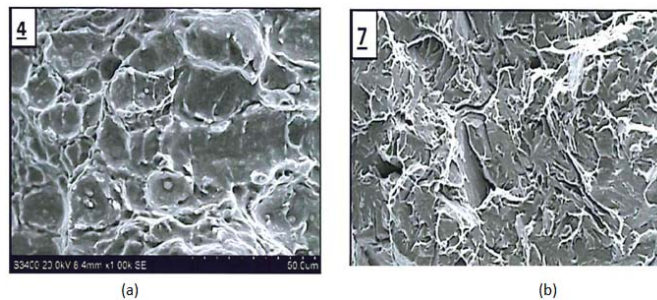


Figure 5: CTOD fractured surface for as-received sample - **a)** Zone corresponding to just ahead of pre-fatigue crack, **b)** Zone corresponding to middle of the specimen

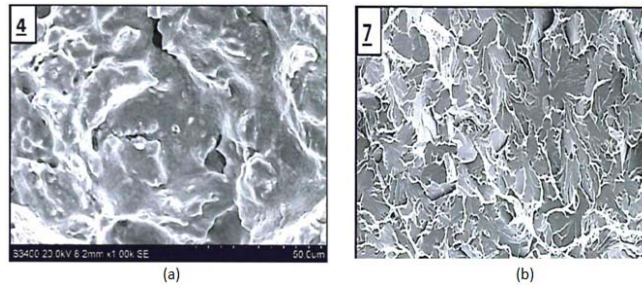


Figure 6: CTOD fractured surface for normalized sample - **a)** Zone corresponding to just ahead of pre-fatigue crack, **b)** Zone corresponding to middle of the specimen

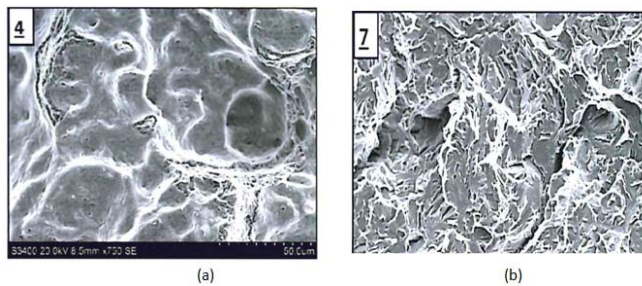


Figure 7: CTOD fractured surface for austempered sample - **a)** Zone corresponding to just ahead of pre-fatigue crack, **b)** Zone corresponding to middle of the specimen

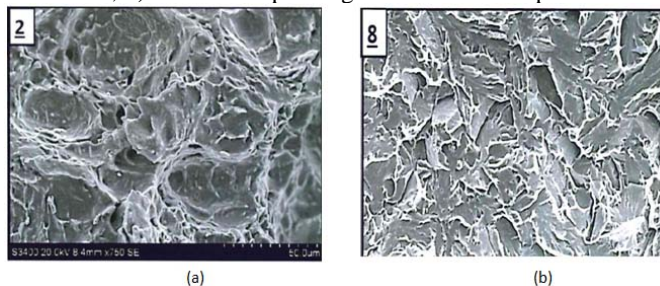


Figure 8: CTOD fractured surface for quenched and tempered sample - **a)** Zone corresponding to just ahead of pre-fatigue crack, **b)** Zone corresponding to middle of the specimen

IV. CONCLUSION

Normalized microstructure has the highest fracture toughness value (0.2263mm), followed by quenched and tempered (0.1265mm), as-received (0.0877mm) and austempered microstructure (0.0546mm). Crack tip opening displacement showed very significant sensitivity to microstructure morphology and therefore remained a useful parameter for predicting fracture toughness of steel since microstructure and fracture correlation exist. Thus, obtained critical CTOD results gave valuable insight to fracture behaviour of high strength steel that will be of great help in the design of structures and materials selection.

REFERENCES

- [1]. E. Billur and T. Altan, Introduction to hot forming. An Article, Hot forming die engineering, 2013.
- [2]. J. Billingham, J. Healy, and H. Bolt, High strength steel- the significance of yield ratio and work hardening for structural performance, Marine Research Review (Pub MTD, 1997).
- [3]. J.E. Ramirez, Characterization of high strength steel weld metals: chemical composition, microstructure, and non-metallic inclusions, Welding Journal, vol.87, 75-S.
- [4]. G. Vukelic and J. Brinc, J-integral as possible criterion in material fracture toughness assessment, Engineering Review, issue 2, 2011, 91 – 96.

- [5]. A. Gopichand, Y. Srinivas and A.V.N.L. Sharma, Computation of stress intensity factor of brass plate with edge crack using J-integral technique, *International Journal of Research in Engineering and Technology*, vol01, 2012, 2319 – 1163.
- [6]. A. Venkert, P.R. Guduru and Kavinchandra, Effect of loading rate of fracture morphology in high strength ductile steel, *Journal of Engineering Materials and Technology*, vol.123, 2001.
- [7]. X. Zhu, J- integral resistance curve testing and evaluation, *Journal of Zhejiang University science A*, 2009,1541-1560.
- [8]. T.L. Anderson, *Fracture mechanics - fundamentals and application* (Third edition, Pub. CRC press, 2005).
- [9]. S.K. Kudari and K.G. Kodancha, On the relationship between J- integral and CTOD for CT and SENB specimen, *Journal on Fracture Mechanics*, Vol 6,2008, 3-10.
- [10]. L.W. Ma, X. Wu and X. Kenong, Microstructure and property of medium carbon steel processed by equal channel angular pressing, *Material forum* Vol. 32, 2008, Pub. Institute of materials engineering Australasia Ltd.
- [11]. S. Al-rubaiey, E. Anon and M.M. Hanoon, The influence of microstructure on the corrosion rate of carbon steel, *Engineering and Technological Journal*, vol.31, 2013, part (A) No 10.
- [12]. ASTM E1820, Standard test method for measurement of fracture toughness (ASTM International USA, 2010)
- [13]. C.A. Reddy, Effect of holding temperature and time for austempering on impact toughness of medium carbon and high alloy steel, *International Journal of Computer Network and Security*, vol 3, 2013.
- [14]. J. Wen, Q. Li and Y. Long, Effect of austempering and mechanical properties of GCr18Mo steel, *Material Science Engineering A*,2006, 251 – 253.
- [15]. H.K.D.H Bhadeshia and Honeycombe , *Steel: microstructure and properties* (3rd Edition, Butterworth-Heinemann, 2006)